Available online at www.CivileJournal.org

Civil Engineering Journal

(E-ISSN: 2476-3055; ISSN: 2676-6957)

Vol. 9, No. 08, August, 2023

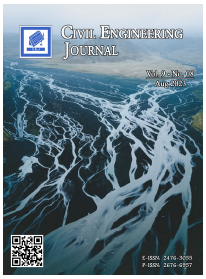

Measuring and Rigidity Moduli of GFRP Experimentally

Youssef A. Awad [1], Ahmed M. El-Fiky [2], Hosam M. Hegazy [1, 3*], Mahmoud G. Hasan [2], Ibrahim A. Yousef [2], Ahmed M. Ebid [1], Mohamed A. Khalaf [2]

[1] *Department of Structural Engineering and Construction Management, Future University in Egypt, Egypt.*

[2] *Structural Engineering Department, Faculty of Engineering, Ain Shams University, Cairo 11517, Egypt.*

[3] *School of Construction Management Technology, Purdue University, West Lafayette, IN, United States.*

Received 30 March 2023; Revised 12 July 2023; Accepted 21 July 2023; Published 01 August 2023

Abstract

Although GFRP poles are widely accepted today due to their low cost and weight and high electrical and corrosion resistance, they suffer large deformations due to the low elastic and rigidity moduli (E & G) values of the GFRP. Accordingly, it is essential to accurately measure these values to estimate the actual deformation of the pole. This study presented a procedure to measure (E & G) values using three different tests on three sample sizes: full, scale pole, conic sample, and ad coupon sample, instead of using the manufacturer values as usual. This study is also concerned with the shear modulus value and when it can be neglected as usual in other traditional materials. The GRG optimization technique was used to analyze the results and determine the optimum values for (E & G) considering the results of the three tests. The results showed that the values of (E & G) are greatly affected by the sample's size and shape, the slenderness ratio of the sample (L/r), and the shear deformation contribution. The critical slenderness ratio (L/r), corresponding to a shear deformation contribution of 10%, was determined for each test. This value is recommended as the upper boundary for any test that measures the (E & G) values. Testing several samples with different (L/r) values is also recommended to enhance accuracy. This study was concerned with determining the optimum values of elastic and rigidity moduli for GRFP poles compared to the manufacturer's conservative values. The results indicated that the shear modulus can be neglected and the importance of the scale effect on the results of flexure and shear modulus.

Keywords: GFRP; Elastic Modulus; Rigidity Modulus; Experimental Measurements; Gradually Reduced Gradient (GRG).

1. Introduction

Fiber-reinforced plastic (FRP) is a great alternative because it has fewer drawbacks than other materials, such as the quick deterioration of wood, the weighty nature of reinforced concrete poles, the short lifespan of aluminum, and the corrosion of steel, which makes treating these materials unprofitable. Transmission networks and electric poles are two examples of crucial infrastructure. FRP has several advantages over materials like steel and aluminum, making it a good choice for transmission and distribution poles, towers, H-frames, and light poles [1]. GFRP has several advantages over conventional steel for meteorological towers, including a high strength-to-weight ratio and corrosion resistance [2]. Although FRP composites have been used for more than 50 years in various applications, other materials, including steel, wood, and aluminum, have been used for considerably longer [3]. The resilience of glass fiber reinforced polymer (GFRP) transmission poles and towers under extreme temperature and UV conditions has been studied. The performance of GFRP material is affected by UV radiation and unfavorable temperature conditions; as a result, the elastic modulus

* Corresponding author: hossam.mostaffa@fue.edu.eg

http://dx.doi.org/10.28991/CEJ-2023-09-08-07

rises, its strength falls, and a little shift in Poisson's ratio occurs [4].

Glass fiber-reinforced plastic (GFRP) poles may be used to build transmission towers, bridge structures, and support transmission lines in place of conventional steel arms, in addition to functioning as force-bearing parts of towers [5]. Utility poles made of glass fiber-reinforced polymer (GFRP) are becoming more common in European countries. Therefore, it is essential to properly inspect the poles' structural properties to guarantee the integrity and safety. Utility poles made of glass fiber-reinforced polymer (GFRP) are becoming more common in European countries [6]. The cost of composite poles is a key obstacle to their international implementation. Another issue that must be avoided is the trash produced by the heavy use of composite material in the future. An electrical outage would create a riskier and more aggressive environment [7]. Damage to light and utility poles located on elevated highways or railroad bridges was seen during several previous earthquakes. They were mainly brought on by mast collapsing, severe pole deformation, yielding-related bending failure, and pole buckling. Poles supporting lighting masts, traffic signs, or transmission cables are essential to improving safety, security, and aesthetics for highway users and surrounding facilities. Among the numerous advantages of switching to FRP composite poles from wood poles is the improvement of road safety by reducing fatalities brought on by auto-pole collisions [8, 9].

The creation of FRP involves several approaches. Centrifugal, pultrusion, and filament winding production techniques frequently provide structural support. From a structural perspective, the manufacturing process can significantly affect the material's structural qualities. The quantity of fiber and the orientation of the glass fibers are additional elements that influence the properties of the FRP laminate. The process produces FRP poles in the oldest and broadest sense. In this procedure, polyester resin-impregnated glass fiber strands are constantly wound around a tapered mandrel using a filament winding machine. Glass fiber strands are twisted on the mandrel in a pre-determined number of windings and at a particular angle. Once the laminate has fully dried, usually with an external heat source, the mandrel is removed. Pultrusion is a mechanical, continuous molding process. The fibers are continuously sucked into a resin bowl, following the design and appropriate sections to be impregnated into the resin tank. The fibers are dragged into the die, heated, and formed in various shapes in the appropriate sector. The product will now be chopped to the appropriate lengths on the table using a cutting saw. Pipes, poles, and tubes are examples of cylindrical objects that respond well to the mechanical centrifugal process. In this procedure, glass fiber is applied to a hollow steel mold designed with various fibers. The resin injection cannon can inject resin into the mold due to the spinning machine's quick rotation (spinning), which spreads the resin evenly throughout the reinforcement. The product usually needs finishing touches, such as cutting the bottom and upper parts and opening the maintenance door, before it is ready for use and doesn't need to be treated. This step is finished with a cutting saw made particularly for these pieces, as shown in Figure 1 [1, 10].

Figure 1. Centrifugal process

The horizontal pole on the ground was fixed using two opposed permanent supports at 0.0 and 1.65 m from the first end. The fixed component of the pole served as a representation of the pole's buried depth, generally calculated as 10% of the pole's length + 600 mm (1.65 m). Two string potentiometers were mounted to each of the two supports to watch for movement and confirm fixation. Next, the pole was vertically loaded 600 mm from the second end using a winch and steel rope. Mechanical transducers were employed to measure the deflection of the FRP pole, and manual controls were used to control the load in the testing device [1, 11].

The pole manufacturer should compute the shaft length using the correct embedment depth (if applicable) and luminaire mounting height. A 61% tolerance must be maintained for the pole's whole length. The pole manufacturer must select the pole's weight to meet the strength requirements of the user's installation. Once the weight has been established, it must be at least 95% of the declared weight. The pole must support at least 1.5 times the maximum bending moment caused by the wind during testing. 15% of the aboveground height is the maximum amount of pole-top deflection that can be brought on by wind action on the pole and any related attachments [12–14].

In 2021, Hamdy demonstrates that replacing carbon fiber with glass fiber on the FRP poles was a good improvement. The total load capacity of the FRP poles and the stiffness increased with increasing the percentage of carbon fiber [15]. Thomas (2021) concluded that it is possible to use the FEM with confidence in the analysis and design of GFRP structures, such as utility line poles and wind turbine towers, without the high cost associated with experimentation [16]. Nawar in 2022 indicated that strengthening the handle door with a steel ring increased the ultimate capacity of the GFRP pole and prevented the fracture of this region. Moreover, the base system became the most effective for pole deformation [17]. Feng in 2021 showed that the straight hollow-section concrete-filled GFRP tube columns generally behaved in a comparable manner before the GFRP tube failure. The outward deformation of the GFRP tube, which was vulnerable in HS-CFGT columns, controlled the failure mode of both straight and tapered columns [18]. The analysis of the literature showed that there is still a gap that has to be filled in order to determine the physical and mechanical properties of the GFRP poles instead of using the manufacturer's values. In order to determine the flexure and shear modulus (E & G), experimental tests were conducted. To test the utility of the GFRP pole, three specimens have been used (full-scale, conic, and coupons).

The main objective of this study is to measure and compare both the elastic and rigidity moduli of GFRP poles by testing three different size samples:

- A full-scale pole;
- A cylindrical segment of the pole (conic sample);
- A strip sample was extracted from the pole (coupon sample).

2. Research Methodology

The research methodology is presented, as shown in Figure 2. The experimental program consists of three phases; 1st phase included testing full-scale pole fixes at the base under concentrated lateral load. The test is repeated three times with different distances between the load and the base. The 2nd phase started by cutting a 1.2-m cylindrical segment from the top of the pole (conic sample) and testing it using the three-point bending test five times for five different spans. Finally, the 3rd phase began with cutting a longitudinal strip from the conic sample (coupon sample) and testing it using the three-point bending test five times for five different spans. It should be noted that full-scale pole and conic samples were tested several times, but within the elastic zone, all deformations were restored after unloading, load-deflection curves were linear, and no cracks or weaknesses were observed.

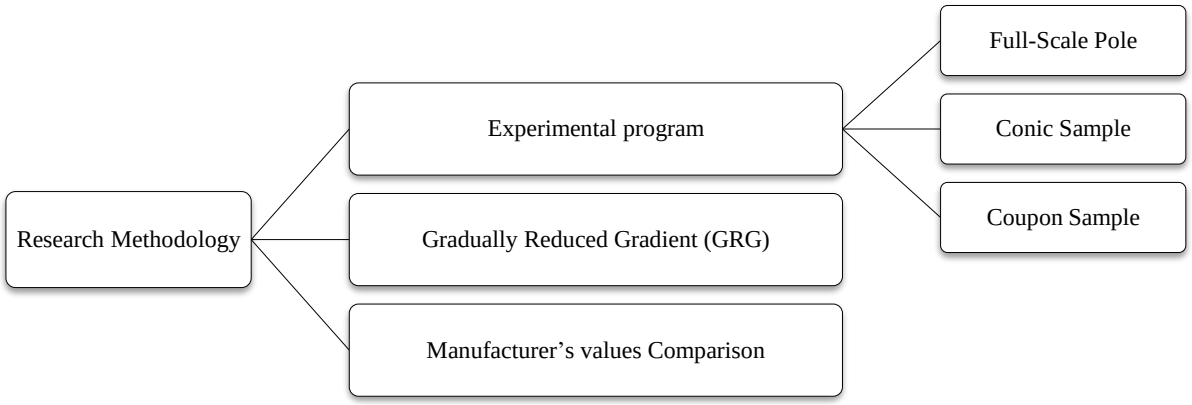

Figure 2. Research Methodology

Loads and corresponding defections were recorded for each test; these readings were analyzed using "Gradually Reduced Gradient (GRG)" to extract the optimum values of both elastic modulus (E) and rigidity modulus (G). Finally, these values were compared with the provided manufacturer's values (20000 & 300 MPa for both elastic and rigidity moduli, respectively).

2.1. Phase 1: Full-Scale Pole

A full-scale GFRP conic poles with constant thickness, manufactured by a centrifugal process with the following dimensions:

- Pole length = 5900 mm;
- Pole diameter at base = 184 mm;
- Pole diameter at top of stub = 174 mm;

- Free end diameter = 76 mm;
- GFRP thickness = 6 mm.

The pole has a 550 mm internal steel stub and is fixed to a concrete block (1200×800×800 mm) by its steel stub base plate (400×400×10 mm) and fixed to a concrete block by 4 bolts 16mm in diameter. A motorized winch (Capacity = 1000 KN) gradually loaded the horizontally fixed pole at different distances from the base. The load is recorded with a load cell, while the deflection is measured manually (E-Metric stick). The first height of the pole is measured from the ground (Y_o) before loading. At failure, height was determined (Y_1. Deflection was calculated by subtracting Y_o from Y_1 ($\Delta = Y_1 - Y_o$). Figure 3 shows the testing setup. Test results are summarized in Table 1 and graphically presented in Figure 4.

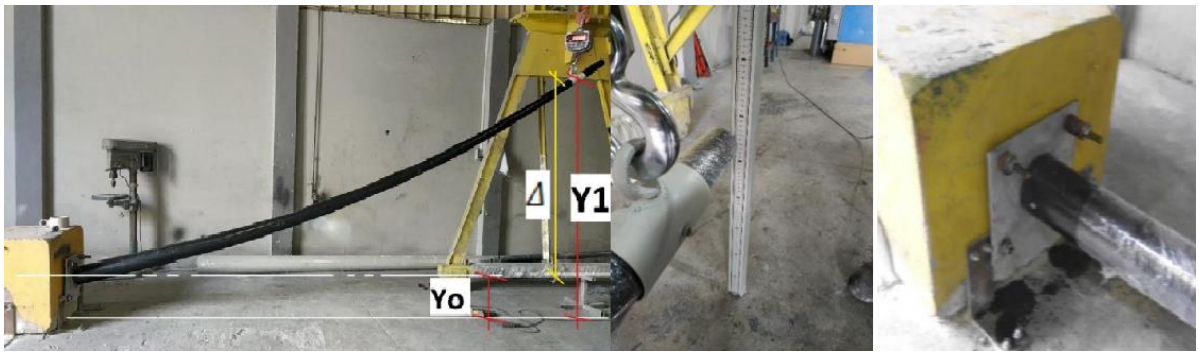

Figure 3. Testing setup of full-scale pole

Table 1. Test results of full-scale pole

Load (N)	Distance from load to internal stub (mm)		
	5100	2850	850
	Deflection at the applied load (mm)		
	Δ1	Δ2	Δ3
1250	170	30	10
2500	340	60	20
3500	490	90	30
4500	640	120	35

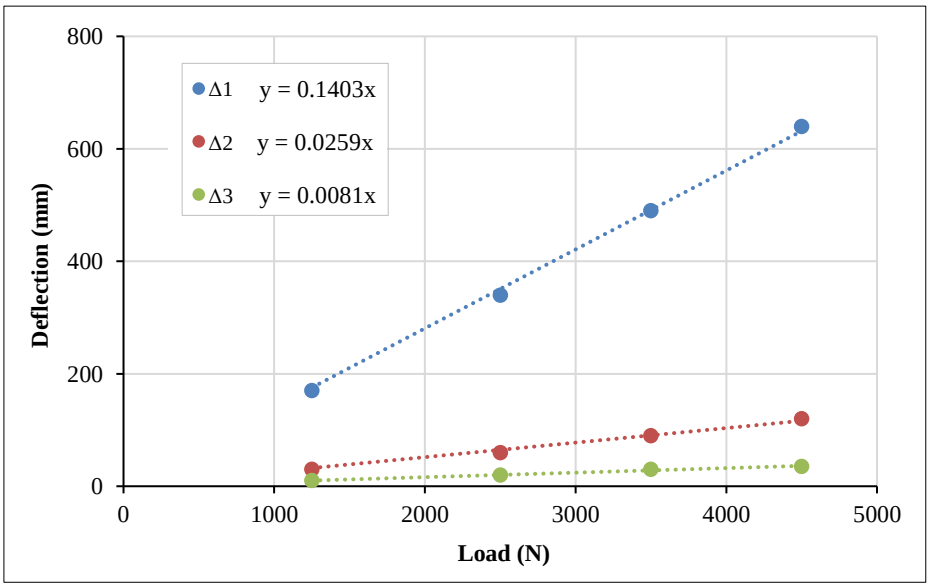

Figure 4. Test results of full-scale pole

Table 2 shows results from our study compared to those from Altanopoulos et al. [16]. Our results using the centrifugal process match well with his results in load but differ in deflection. The error is 48% for the stiffness result. We note that Thomas in 2021 used a pole manufactured using the filament winding process with different dimensions,

mechanical properties, and fixation methods. The error can be attributed to that reason. We concluded that the different manufacturing processes and properties will differ in results, and it is recommended to use them for further studies to compare results.

Table 2. Comparison study

Parameters	Results	Thomas 2021 results	$(\frac{Results}{Thomas\ 2021})$ %
Load	4500 N	4050 N	112
Deflection	640 mm	300 mm	214
Stiffness	7 N/mm	13 N/mm	54
E	36 GPa	45 GPa	80
G	1.20 GPa	4.80 GPa	25
Pole Thickness	6 mm	3 mm	200
Manufacturing Process & Fiber Volume Fraction	Centrifugal & 65%	Filament Winding & 50%	-

2.2. Phase 2: Conic Sample

A piece of 1200 mm length was cut from the top of the pole. The sample diameters at both ends were 104 and 76 mm. This sample was tested five times using the three-point bending test with different spans, as shown in Figure 5. Both load and the corresponding deflection were recorded, as summarized in Table 3 and illustrated in Figure 6.

Figure 5. Testing the conic sample

Table 3. Test results of conic sample

Load (N)	Span (mm)				
	270	450	630	810	990
	Deflection at mid-span (mm)				
	Δ1	Δ2	Δ3	Δ4	Δ5
500	0.051	0.220	0.353	0.410	0.530
1000	0.100	0.400	0.705	0.720	1.000
1500	0.152	0.620	1.051	1.000	1.510
2000	0.200	0.780	1.420	1.730	2.000
2500	0.251	1.025	1.740	1.810	2.160

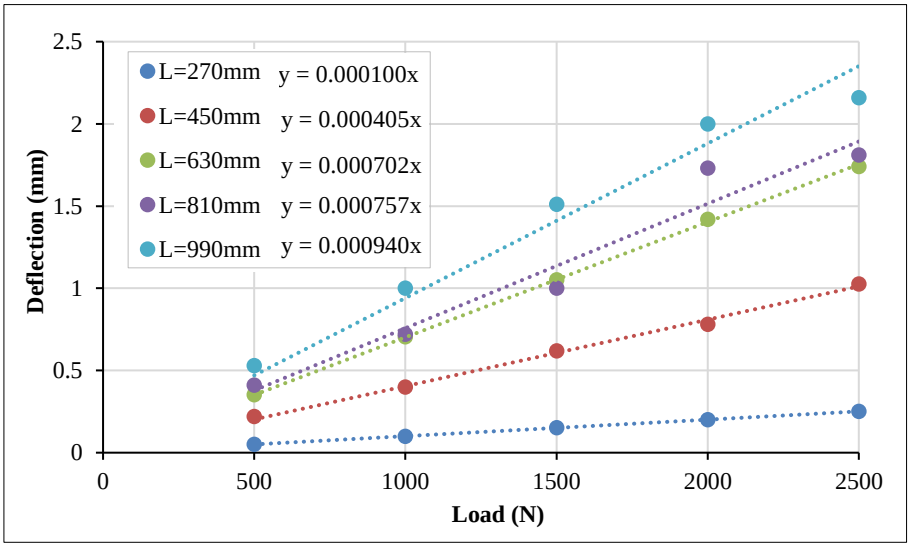

Figure 6. Test results of conic sample

2.3. Phase 3: Coupon Sample

Five strips (coupons) (240×30×6mm) were cut out from the pole and tested at different spans using the three-point bending test as per ASTM (D 790 – 03). The setup test is shown in Figure 7. All recorder loads and deformations are listed in Table 4 and presented in Figure 8.

(a) Coupon samples (b) Testing setup

Figure 7. Testing the coupon sample

Table 4. Test results of coupon samples

Load (N)	Span (mm)				
	18	30	42	54	66
	Deflection at mid-span (mm)				
	Δ1	Δ2	Δ3	Δ4	Δ5
500	0.014	0.046	0.076	0.091	0.224
1000	0.031	0.089	0.160	0.170	0.449
1500	0.046	0.134	0.225	0.270	0.680
2000	0.059	0.189	0.290	0.370	0.910
2500	0.076	0.224	0.374	0.449	1.126

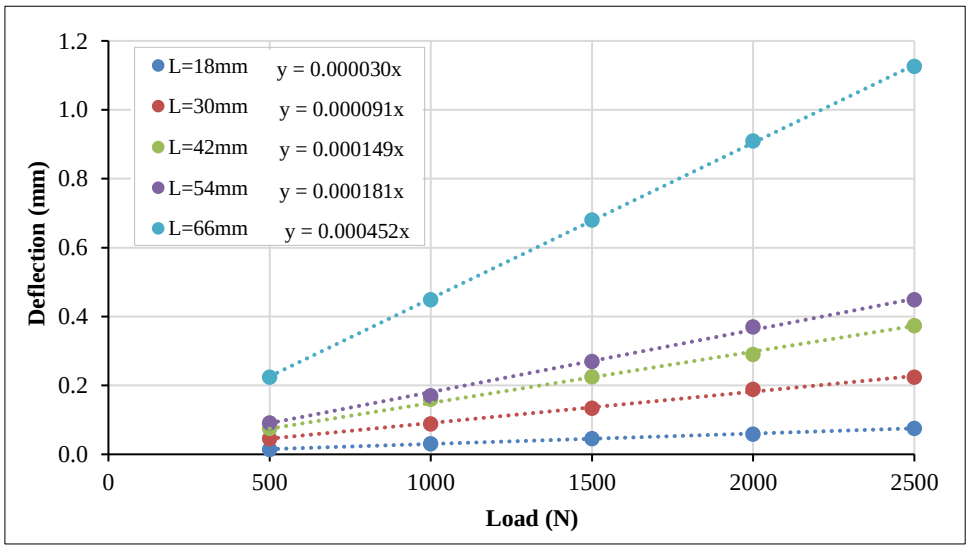

Figure 8. Test results of coupon samples

3. Analysis and Discussions

3.1. Main Findings

The word cloud of the literature review for the retrieved publications' trend in publishing and abstract is shown in Figure 9.

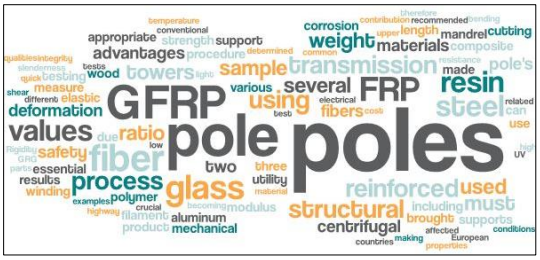

Figure 9. Visualization for keywords by Pro Word Cloud

The tested pole acted as a cantilever beam with a concentrated load at the tip; hence, its deflection could be calculated using Equation 1 from beam theory [19], while the conic and coupon samples acted as simple beams with a concentrated load at mid-span; hence, its deflection could be calculated using Equation 2.

$$\Delta = \frac{PL^3}{3E.I} + \frac{PL}{G.Ar} \quad (1)$$

$$\Delta = \frac{PL^3}{48E.I} + \frac{PL}{4G.Ar} \quad (2)$$

where E is the elastic modulus of the GRFP, G is the rigidity modulus of the GRFP, Ar is the reduced cross-section area of a sample (50% & 83% of the gross area (A) for pipes & rectangle section respectively), I is the moment of inertia of the cross-section of the sample, and L is the sample span.

The analysis started with calculating the theoretical deflection values for the three samples under the considered loading conditions using the manufacturer's recommended values for (E & G) and calculating the "Mean Absolute Relative Error" (MARE) for each sample as per Equation 3.

$$\text{MARE} = \frac{\sum\left|\frac{\Delta th - \Delta exp}{\Delta exp}\right| \times 100}{n_{samples}} \quad (3)$$

A built-in optimization module in MS-EXCEL software called "Solver" was used to minimize the (MARE) value using the (GRG) technique. (GRG) is a well-known mathematical technique used to optimize functions by gradually changing the values of their parameters one by one while observing the output and the constraining conditions (if any). In this case, (GRG) was used to find the optimum values for (E & G) that minimize the (MARE). (MARE) was selected as a target for the optimization process instead of the traditional "Sum of Squared Error" (SEE) or "Mean Absolute Error" (MAE) because of the large variations in deflection magnitude between different tests (from 0.014 mm to 640 mm). The optimum (E & G) values for each sample and all samples are listed in Table 5 along with the corresponding (MARE). The relations between the theoretical and experimental deflection values are illustrated in Figure 10.

Table 5. Optimum (E & G) values

Sample	(E) MPa	(G) MPa	MARE
Full-scale pole	43024	73	22.7%
Conic sample	19432	980	22.5%
Coupon samples	30549	1287	15.3%
All Samples	**31239**	**940**	**27.8%**

3.2. Comparison with Other Studies

Comparing the calculated stiffness characteristics values with other research [20] showed good agreement; the calculated stiffness characteristics values (E & G) ranged between 78% and 156% of the compared ones. This difference is expected due to differences in geometric properties and the fixation method of the pole, as shown in Table 6.

Table 6. A Comparison Study of Stiffness Characteristics

Parameter	Calculated	Salib & Abdel-Sayed (2012) [20]	$(\frac{Calculated}{Salib\ 2011})$ %
Flexure Modulus (MPa)	31239	40000	78
Shear Modulus (MPa)	940	600	156

3.3. Finding Explanation

As shown in Table 4, the optimum values for (E & G) are (31250 & 940 MPa), which are higher than the recommended values by the manufacturer. (E/G) the ratio is 33.3, within the common range (5 to 40). From Equations 1 and 2, it could be noted that as the slenderness ratio (L/r) value increased, the contribution of shear deformations ($\Delta_{sh}/\Delta_{total}$) decreases, where (r) is the radius of gyration. Generally, the shear deformations could be neglected if its contribution is less than 10% of the total deformation. The critical (L/r) ratio could be determined by substituting in Equations 1 and 2 with ($r = \sqrt{I/A}$) which leads to Equations 4 and 5.

$$\frac{L}{r} = \sqrt{\frac{9\times 3E}{(\frac{Ar}{A})\,G}} \qquad \textit{For cantilever beam} \tag{4}$$

$$\frac{L}{r} = \sqrt{\frac{9\times 48E}{(\frac{Ar}{A})\,G}}\sqrt{\frac{E}{G}} \qquad \textit{For simple beam} \tag{5}$$

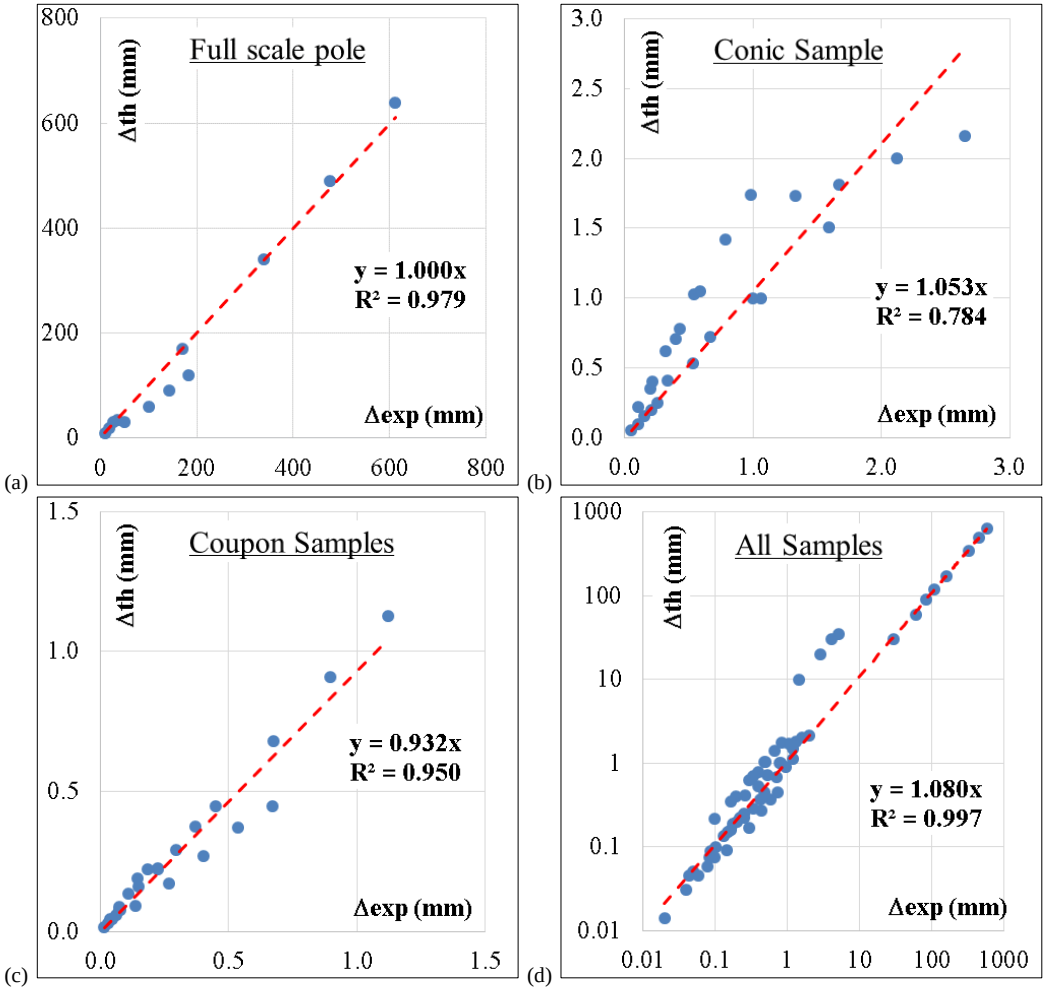

Figure 10. The relations between the theoretical and the experimental deflection values, a) Full-scale pole, b) conic sample, c) Coupon samples, and d) all samples

In the case considered in this study, (E/G) =33.3. Hence, it could be concluded that the shear deformation contribution could be neglected if (L/r > 40) for cantilever pipe (full-scale pole), (L/r > 170) for supported pipe (conic samples), and (L/r > 130) for supported rectangular section beam (coupon sample).

4. Conclusions

This study was concerned with determining the optimum values of elastic and rigidity moduli for GRFP using three experimental tests: full scale pole, conic sample, and coupon sample. In addition, the results were annualized using the GRG technique. Therefore, the results of the study could be summarized as follows:

- The three considered experimental tests to measure the values of (E) & (G) gave very different values due to size effects and shear deformation contributions. The optimum measured values considering all the results were (31250 & 940 MPa) for (E & G) respectively.
- A comparison study has been presented between the experimental study and previous research, showing an agreement in E & G by 78% and 156%, respectively.

- Full-scale pole tests' results were overestimated for the (E) value and underestimated for the (G) value because two of the three tests had (L/r > 40), and hence the deformations were mainly governed by the flexural behavior. Accordingly, the measured low value of (G) was compensated by the high value of (E).
- On the opposite, conic samples showed the lowest value of (E) and a fair value of (G) because the (L/r) values ranged between 9 and 32, which is much less than 170; accordingly, the shear deformation contributions were significant.
- Finally, the coupon sample results presented the closest value for (E) and overestimated the (G) value. As a result, the (L/r) values for the tested samples were low (ranging between 11 and 38) compared with the limit of 130.
- This research work improves the stiffness characteristics results by using different techniques, which will lead other researchers to use different values of E & G to improve their findings and to know when the shear modulus can be neglected.

5. Declarations

5.1. Author Contributions

Conceptualization, A.M.E. and M.A.K.; methodology, Y.A.A.; software, Y.A.A.; validation, H.M.E., M.G.H., and I.A.-L.; formal analysis, Y.A.A.; investigation, H.M.E., M.G.H., and I.A.-L.; resources, A.M.E.; data curation, A.M.E.; writing—original draft preparation, Y.A.A. and A.M.E.-F.; writing—review and editing, A.M.E. and H.M.E.; visualization, M.G.H. and I.A.- L.; supervision, M.A.K.; project administration, M.A.K.; funding acquisition, Y.A.A. All authors have read and agreed to the published version of the manuscript.

5.2. Data Availability Statement

The data presented in this study are available in the article.

5.3. Funding

This study is sponsored by Future University in Egypt, Cairo, Egypt.

5.4. Conflicts of Interest

The authors declare no conflict of interest.

6. References

[1] EL-Fiky, A. M., Awad, Y. A., Elhegazy, H. M., Hasan, M. G., Abdel-Latif, I., Ebid, A. M., & Khalaf, M. A. (2022). FRP Poles: A State-of-the-Art-Review of Manufacturing, Testing, and Modeling. Buildings, 12(8), 1085. doi:10.3390/buildings12081085.

[2] Alshurafa, S., Alnaafa, M. A., & Polyzois, D. (2022). Development of GFRP Guyed Communication Towers. 10th International Conference on FRP Composites in Civil Engineering, CICE 2021, Lecture Notes in Civil Engineering, 198, Springer, Cham, Switzerland. doi:10.1007/978-3-030-88166-5_164.

[3] Zhang, L., Sun, Q., & Zheng, L. (2011). Experimental study on the durability of Glass Fiber Reinforced Polymer Pole and Tower for power transmission. Advanced Materials Research, 168–170, 1717–1724. doi:10.4028/www.scientific.net/AMR.168-170.1717.

[4] Sheridan, R., Gilman, J. W., Busel, J. P., Hartman, D., Holmes, G., Coughlin, D., Kelley, P., O'Donnell, W. R., Nanni, A., Troutman, D., Harris, R. W., Gutierrez, J., Bakis, C., Holmes, S., Moser, R., Lackey, E., Fekete, J., Watson, S., Kim, J.-H., … Natarajan, B. (2017). Road mapping workshop report on overcoming barriers to adoption of composites in sustainable infrastructure, National Institute of Standards and Technology Special Publication 1218. doi:10.6028/nist.sp.1218.

[5] Si, J., Qiu, S., Feng, S., Chen, J., & Wang, Z. (2022). Experimental study on axial compression buckling of glass fiber reinforced plastics solid pole with circular cross-section. Advances in Structural Engineering, 25(4), 913–924. doi:10.1177/13694332211054226.

[6] Broniewicz, M., Broniewicz, F., & Broniewicz, E. (2021). A full-scale experimental investigation of utility poles made of glass fibre reinforced polymer. Materials, 14(23), 7398. doi:10.3390/ma14237398.

[7] Tripathi, S., Gupta, S., Kumar, V., & Tiwari, P. (2020). Hybrid Utility Poles and their application in Power System: Refinement in Construction and Design of Conventional Utility Pole. International Conference on Electrical and Electronics Engineering, ICE3 2020, 606–611. doi:10.1109/ICE348803.2020.9122824.

[8] Siringoringo, D. M., Fujino, Y., Nagasaki, A., & Matsubara, T. (2021). Seismic performance evaluation of existing light poles on elevated highway bridges. Structure and Infrastructure Engineering, 17(5), 649–663. doi:10.1080/15732479.2020.1760894.

[9] GangaRao, H. (2017). Infrastructure Applications of Fiber-Reinforced Polymer Composites. Applied Plastics Engineering Handbook, 675–695, William Andrew, Norwich, United Kingdom. doi:10.1016/b978-0-323-39040-8.00032-8.

[10] Fouad, F. H., & Mullinax, Jr., E. C. (2000). FRC Poles for Distribution Power Lines. Advanced Technology in Structural Engineering, 1-7. doi:10.1061/40492(2000)179.

[11] Abdelkarim, O. I., Guerrero, J. M., Mohamed, H. M., & Benmokrane, B. (2019). Behaviour of Pultruded Glass Fibre-Reinforced Polymer Utility Poles Under Lateral Loads. Proceedings of the CSCE Annual Conference, 12-15 June, 2019, Laval, Canada.

[12] Yen, H. C. (2010). Method of manufacturing a fiber reinforced plastic (FRP) lighting pole. U.S. Patent Application No. 12/314,800.

[13] Polyzois, D., Raftoyiannis, I. G., & Ibrahim, S. (1998). Finite elements method for the dynamic analysis of tapered composite poles. Composite Structures, 43(1), 25–34. doi:10.1016/S0263-8223(98)00088-9.

[14] Abdel Aziz, Y. H., Abdel Zaher, Y., Wahab, M. A., & Khalaf, M. (2019). Predicting temperature rise in Jacketed concrete beams subjected to elevated temperatures. Construction and Building Materials, 227, 116460. doi:10.1016/j.conbuildmat.2019.07.186.

[15] M. Mohamed, H. (2021). Finite Element Modeling of CFRP Composite Pole Structures. International Journal of Engineering Applied Sciences and Technology, 6(7), 10–15. doi:10.33564/ijeast.2021.v06i07.003.

[16] Altanopoulos, T. I., Raftoyiannis, I. G., & Polyzois, D. (2021). Finite element method for the static behavior of tapered poles made of glass fiber reinforced polymer. Mechanics of Advanced Materials and Structures, 28(20), 2141–2150. doi:10.1080/15376494.2020.1717691.

[17] Nawar, M. T., Kaka, M. E., El-Zohairy, A., Elhosseiny, O., & Arafa, I. T. (2022). Effect of Supporting Base System on the Flexural Behavior and Toughness of the Lighting GFRP Poles. Sustainability (Switzerland), 14(19), 2614. doi:10.3390/su141912614.

[18] Feng, B., Zhu, Y.-H., Xie, F., Chen, J., & Liu, C.-B. (2021). Experimental Investigation and Design of Hollow Section, Centrifugal Concrete-Filled GFRP Tube Columns. Buildings, 11(12), 598. doi:10.3390/buildings11120598.

[19] Ghugal, Y. M., & Sharma, R. (2011). A refined shear deformation theory for flexure of thick beams. Latin American Journal of Solids and Structures, 8(2), 183–195. doi:10.1590/s1679-78252011000200005.

[20] Salib, S., & Abdel-Sayed, G. (2012). Dynamic behaviour and seismic response of FRP light poles in high seismic zones. Proceedings of the 6th International Conference on FRP Composites in Civil Engineering, 13-15 June, 2012, Rome, Italy.